

# Bottom-up Design of Hydrogels through Click-Chemistry Modification of Magnetic Nanoparticles

Ilaria Meazzini<sup>†</sup>, Massimo Bonini, Francesca Ridi\*, Piero Baglioni

*Department of Chemistry "Ugo Schiff" & CSGI, University of Florence, via della Lastruccia 3, Sesto Fiorentino (FI), 50019, Italy*

\*Corresponding author: Tel: (+39) 0554573015; E-mail: francesca.ridi@unifi.it

<sup>†</sup>Present address: School of Chemistry, Trinity College, The University of Dublin, College Green, Dublin 2, Ireland

Received: 13 August 2018, Revised: 21 September 2018 and Accepted: 20 November 2018

DOI: 10.5185/amlett.2019.2214

www.vbripress.com/aml

## Abstract

The paper describes a modular approach based on click chemistry for the surface modification of magnetic oxide nanoparticles and their covalent inclusion within chemical hydrogels. As a proof of concept, we prepared cobalt ferrite nanoparticles and we modified their surfaces through the reaction with molecules bearing a carboxylic function and, alternatively, either an azide or an alkyne moiety. In the second step, the modified nanoparticles were reacted through a Huisgen 1, 3-dipolar cycloaddition with a molecule bearing an unsaturated function and either an alkyne or an azide moiety, respectively. Finally, the particles were successfully copolymerized with acrylamide and N, N'-methylenebisacrylamide to obtain a magnetically responsive hydrogel. This approach could be easily extended towards any type of inorganic oxide nanoparticles and their inclusion within any radically co-polymerized hydrogel. Copyright © VBRI Press.

**Keywords:** Polymeric nanocomposite, magnetic nanoparticles, click-chemistry, polyacrylamide gel, responsive materials.

## Introduction

Polymer-based inorganic nanoparticle composites are increasingly used to generate functional and responsive materials, thanks to the combination of the stability and process ability of polymers with the peculiar properties of the inorganic nanoparticles. Recent reviews have highlighted how different strategies could successfully produce smart composites, where the interaction between particles' surface and polymeric matrix is crucial to regulate the material's functionalities [1, 2]. In particular, the inclusion of magnetic nanoparticles in composite materials is of particular interest, as it allows for the introduction of responsiveness to static and alternating magnetic fields, that can be exploited in a number of applications, such as environmental remediation [3, 4] drug release, [5-12] bone tissue engineering, [13] conservation of works of art, [14, 15] and hyperthermia [16].

When designing a polymeric nanocomposite, the surface functionalization of the inorganic particles is a critical issue: in fact, identifying effective and selective functionalization methods provides chemists with a "toolbox" for regulating the interaction between the particle and the polymer, which eventually regulates the behaviour of the composite while functioning. In this perspective, both covalent and non-covalent interactions

represent viable strategies. Learning from Nature, the use of non-covalent interactions provides the unique advantage of obtaining self-healing materials: in fact, thanks to the low energies involved, the system is able to take advantage of thermal energy to spontaneously reduce the number and extension of defects, so to minimize its free energy, leading to the formation of highly ordered and predictable systems. On the other hand, the disadvantage of using non-covalent interactions is that the functionalization of the surface is "weak" (*i.e.*, functionalized particles coexist with naked particles plus the functionalizing molecule) and can be affected by subtle variations of factors such as concentration, temperature, pH or ionic strength.

The use of covalent interactions, while not allowing for the preparation of materials with a degree of order comparable to the non-covalent approach, allows for the preparation of robust materials, also with multi-step sequential methods. An extremely simple process to covalently modify the surface of the material, is provided by the *click chemistry* approach [17]. According to the principles delineated by Sharpless, a *click chemistry* reaction must be modular, give high yields, use harmless products that can be removed by non-chromatographic methods, be stereospecific, of simple experimental set-up, can be carried out with reagents and materials readily available and without the use of solvents or at least

conducted with not harmful solvents (water is ideal) and easily removable [18].

In this framework, the use of magnetic nanoparticles as building block is of great help as it introduces the possibility to magnetically separate the reaction products. Furthermore, iron-based oxide nanoparticles show a marked reactivity in water (especially in alkaline conditions) towards carboxylic groups [19].

In this paper, we describe a bottom-up strategy for the inclusion of magnetic nanoparticles in a polyacrylamide gel, thanks to the chemical functionalization of the particles' surface and exploiting the Huisgen 1,3-dipolar cycloaddition, that is one of the typical *click chemistry* reactions [17, 20]. To highlight the modularity and tunability of this approach, nanoparticles' surface was first functionalized with a molecule bearing a carboxylic group and either an azide or a terminal alkyne moiety. This reaction was followed by the 1, 3-dipolar cycloaddition with a molecule bearing a terminal alkyne or an azide, respectively, as well as an unsaturated function (a double bond) which is then used to copolymerize the functionalized nanoparticles with an acrylamide-based hydrogel. We have chosen to demonstrate the suitability of this synthetic strategy (sketched in Fig. 1) as the procedure is extremely simple and it can be easily extended to different polymeric composite materials by changing the molecules used for the second step of the synthesis, as long as they contain a terminal alkyne or an azide moiety to react through a Huisgen reaction and they possess the right chemistry to ensure the proper reactivity and/or interaction with the polymeric matrix.

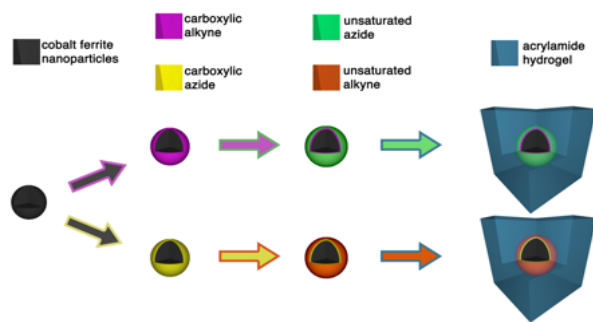


Fig. 1. Sketch of the synthetic strategy for the bottom-up modular preparation of acrylamide-based magnetic hydrogel.

## Experimental

### Materials

Iron (III) chloride hexahydrate ( $\text{FeCl}_3 \cdot 6\text{H}_2\text{O}$ , 97%), iron nitrate ( $\text{Fe}(\text{NO}_3)_3 \cdot 9\text{H}_2\text{O}$ , 98%), Tetramethyl ammonium chloride ( $(\text{CH}_3)_4\text{NCl}$ , 97%) and nitric acid ( $\text{HNO}_3$ , 90%) were purchased from Sigma-Aldrich. Cobalt(II) nitrate hexahydrate ( $\text{Co}(\text{NO}_3)_2 \cdot 6\text{H}_2\text{O}$ , 99%), tetramethylammonium hydroxide ( $(\text{CH}_3)_4\text{NOH}$ , 25% wt solution in water) and sodium hydroxide ( $\text{NaOH}$ , 99%) were purchased from Fluka. 4-azido benzoic acid (98%) and 3-(4-azidofenil)-2-propenal (>98%) were provided by ABCR GmbH. Acrylamide (98%), N,N'-

Methylenebisacrylamide (98%) and 3-methyl-1-penten-4-yn-3-ol (98%) were purchased from Aldrich. DL-Propargylglycine was purchased from Sigma.

### Synthesis of the nanoparticles

The synthesis of magnetic nanoparticles (MagNPs) was carried out using a modified Massart method, described in details in the literature [21]. Briefly, five solutions were prepared, as described in table 1. Solutions A and B were added to 0.5 ml of concentrated nitric acid. This mixture and solution C were separately warmed to the boiling point and then mixed under vigorous agitation. The boiling temperature and the agitation were maintained for 2 hours and then the black precipitate was separated from the supernatant by magnetic decantation and washed with water. The precipitate was separated again by magnetic decantation and dispersed in a 2 M  $\text{HNO}_3$  solution. This mixture was kept under vigorous agitation for 30 min; the precipitate was isolated again by magnetic decantation, and then dispersed during 1h in a mixture of solutions D and E, already at the boiling temperature. The precipitate obtained after this treatment was isolated, washed once with a 1 M  $\text{HNO}_3$  solution and twice with acetone, and then re-dispersed in 5 mL of water. Residual acetone was removed by rotavapor, finally obtaining a stable suspension of positively charged  $\text{CoFe}_2\text{O}_4$  nanoparticles with concentration of 5% wt and average radius of 4 nm [21].

Table 1. Solutions used to prepare the magnetic nanoparticles.

Solution	Salt	Amount	Volume	Conc.
		t		
A	$\text{FeCl}_3 \cdot 6\text{H}_2\text{O}$	4.32 g	16 ml	1 M
B	$\text{Co}(\text{NO}_3)_2 \cdot 6\text{H}_2\text{O}$	2.33 g	8 ml	1 M
C	$\text{NaOH}$	4.00 g	100 ml	1 M
D	$\text{Fe}(\text{NO}_3)_3 \cdot 9\text{H}_2\text{O}$	2.83 g	14 ml	0.5 M
E	$\text{Co}(\text{NO}_3)_2 \cdot 6\text{H}_2\text{O}$	1.02 g	7 ml	0.5 M

### Characterization techniques

ATR-FTIR measurements were performed on a Nexus 870 spectrometer (Nicolet, Madison, WI, USA), equipped with a liquid  $\text{N}_2$ -cooled mercury cadmium telluride (MCT) detector (650–4000  $\text{cm}^{-1}$  range, resolution 2  $\text{cm}^{-1}$ ).

Thermogravimetric analyses (TGA) was conducted on a SDT Q600 (TA Instruments, Newcastle, DE, USA) from room temperature to 1000 °C at 10 °C/min.

Morphological characterization was conducted by means of scanning electron microscopy (Leica Cambridge Stereoscan S360) on freeze-dried samples, coated with gold by sputtering.

Differential Scanning Calorimetry (DSC) was performed on a DSC Q2000 (TA Instruments, Newcastle, DE, USA): the gel samples were freeze-dried and then re-hydrated in excess of milliQ water. Roughly 20 mg of these samples were closed in aluminum hermetic pans and subjected to the DSC analysis, with this experimental program: ramp from RT to -90 °C, at 1 °C/min; ramp from -90 °C to RT at 1 °C/min.

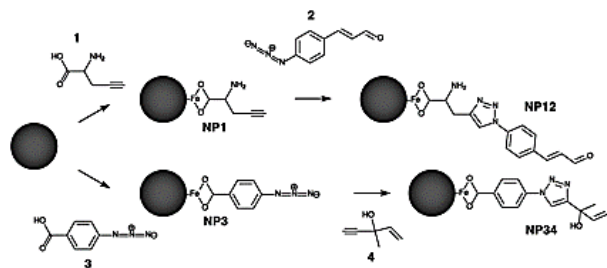


Fig. 2. Scheme of the reactions carried out to modify the surface of magnetic nanoparticles.

## Results and discussion

The synthetic approach to modify the surface chemistry of magnetic nanoparticles (MagNPs) is sketched in Fig. 2, and described step by step hereinafter.

### Synthesis of NP1:

This step includes the functionalization of the surface of the MagNPs with the alkyne **1** to obtain the product **NP1** which is then reacted with the azide **2** to obtain **NP12**. In particular, 11 mL of a water solution (1% wt) of DL-Propargylglycine (**1**) and 1.5 mL of  $(\text{CH}_3)_4\text{NOH}$  (25% wt solution in water) were added to 200  $\mu\text{L}$  of MagNPs suspension (5% wt in water). The dispersion was mechanically mixed during few hours and then the modified MagNPs were collected with the aid of a permanent magnet (NdFeB, around 1 T) and analysed by means of ATR-FTIR. The comparison between the infrared spectra of reactant and product (see Supplementary materials, Fig. S1) clearly show that the functionalization has successfully taken place: in fact, the results indicate that **1** reacts with the surface of MagNPs thanks to the carboxylic moiety, as confirmed by the changes in the ATR-IR spectrum in the region between 1750 and 1500  $\text{cm}^{-1}$ . Please note that an alkaline environment and the consequent negative charge of then particles' surface is needed to promote the reaction: in fact, without the addition of  $(\text{CH}_3)_4\text{NOH}$ , the reaction takes place only to a minor extent.

### Synthesis of NP12:

This step includes the reaction of **NP1** with the azide **2** to obtain **NP12**. In particular, the product **NP1** (before being separated from the reaction medium) was added with 2.2 mg of 3-(4-azidofenil)-2-propenal (**2**) in 10 mL of ethanol (reactant **2** is not soluble in water), 0.15 mg of  $\text{CuSO}_4 \cdot 5\text{H}_2\text{O}$ , 0.22 mg of ascorbic acid and 17 mL of  $\text{H}_2\text{O}$  (MilliQ grade). The reaction was carried out at 50°C during 3 days. The magnetic product was collected with the aid of a permanent magnet (NdFeB, around 1 T), dried and analysed by means of ATR-FTIR. Taking into account that the Huisgen reaction takes to the formation of a 1, 2, 3-triazole cycle, the diagnostic signals for a successful preparation of **NP12** would be the absence of: C-H stretching absorption typical of alkynes between 3330 and 3260  $\text{cm}^{-1}$ , the absence of CC triple bond absorption around 2520  $\text{cm}^{-1}$ , and the absence of N=N=N stretching absorption typical of azides between 2200 and 2100  $\text{cm}^{-1}$ . All these signals have disappeared in the

spectrum of **NP12** (Fig. S2), confirming its preparation. The sample was also characterized by TGA (Fig. S3), showing that the organic content in the final product is about 22 % wt.

### Synthesis of NP3

This step includes the functionalization of the surface of the MagNPs with the azide **3** to obtain the product **NP3** which is then reacted with the alkyne **4** to obtain **NP34**. In particular, 5 mL of an acetone solution (1% wt) of 4-azido benzoic acid (reactant **3** is not soluble in water) and 1.5 mL of  $(\text{CH}_3)_4\text{NOH}$  (25% wt solution in water) were added to 200  $\mu\text{L}$  of MagNPs suspension (5% wt in water). The dispersion was mechanically mixed during and the magnetically collected product was analysed by means of ATR-FTIR and TGA. The comparison between the infrared spectra of reactant and product (see Supplementary materials, Fig. S4) clearly show that the functionalization has successfully taken place. The addition of  $(\text{CH}_3)_4\text{NOH}$  is needed also in this case for the same reasons discussed in the synthesis of **NP1**.

### Synthesis of NP34:

This step includes the reaction of **NP3** with the alkyne **4** to obtain **NP34**. In particular, the product **NP3** (before being separated from the reaction medium) was added with 10  $\mu\text{L}$  of 3-methyl-1-penten-4-yn-3-olo (**4**) in 6.6 mL of acetone (reactant **4** is not soluble in water), 0.15 mg of  $\text{CuSO}_4 \cdot 5\text{H}_2\text{O}$ , 0.22 mg of ascorbic acid and 17 mL of  $\text{H}_2\text{O}$  (MilliQ grade). The reaction was carried out at 50 °C during 3 days and the magnetic product was magnetically collected, dried and analysed by means of ATR-FTIR. Following the same arguments discussed in the previous paragraph, the spectrum of the product (Fig. S5) confirms the successful preparation of **NP34**. The sample was also characterized by TGA (Fig. S6), showing that the organic content in the final product is about 39% wt.

### Preparation of hydrogels:

Reference acrylamide-based hydrogel (**GEL**) was prepared through radical copolymerization of a water solution (10 mL) containing 0.6g of acrylamide and 75mg of N, N'-methylene-bisacrylamide, added with few milligrams of  $(\text{NH}_4)_2\text{S}_2\text{O}_8$  (as the radical starter) and then placed at 42°C in a sonication bath (Labsonic LBS2-4 operating at 60 kHz, Falc Instruments, Italy). The functionalized nanoparticles (**NP12** and **NP34**) were embedded in the hydrogel matrix by preparing a water dispersion (concentration about 8% wt) through sonication.

These dispersions were alternatively mixed with the same solutions used to prepare the reference hydrogel, in a 1:2 volume ratio, and then copolymerized under sonication to obtain a hydrogel containing either **NP12** particles (**NP12GEL**) or **NP34** particles (**NP34GEL**). The visual appearance of the obtained hydrogels is shown in Fig. 3, clearly displaying that magnetic nanoparticles tend to settle during the

copolymerization. This can be easily exploited to obtain hydrogel with a different magnetic concentration: in fact, hydrogel slices can be easily obtained by cutting the hydrogel with a laboratory blade. In our investigation, we focused on the phase formed at the bottom (*i.e.*, with higher magnetic content).

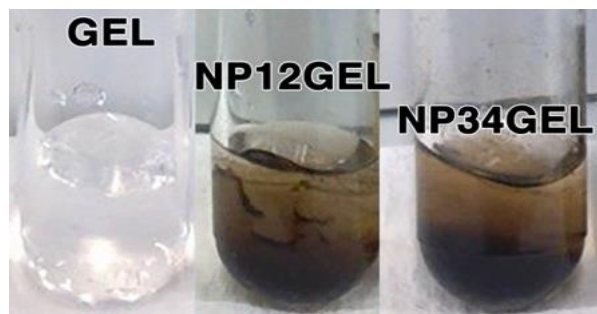


**Fig. 3.** Visual appearance of the hydrogels obtained without magnetic nanoparticles (GEL), with NP12 magnetic nanoparticles (NP12GEL) and with NP34 magnetic nanoparticles (NP34GEL).

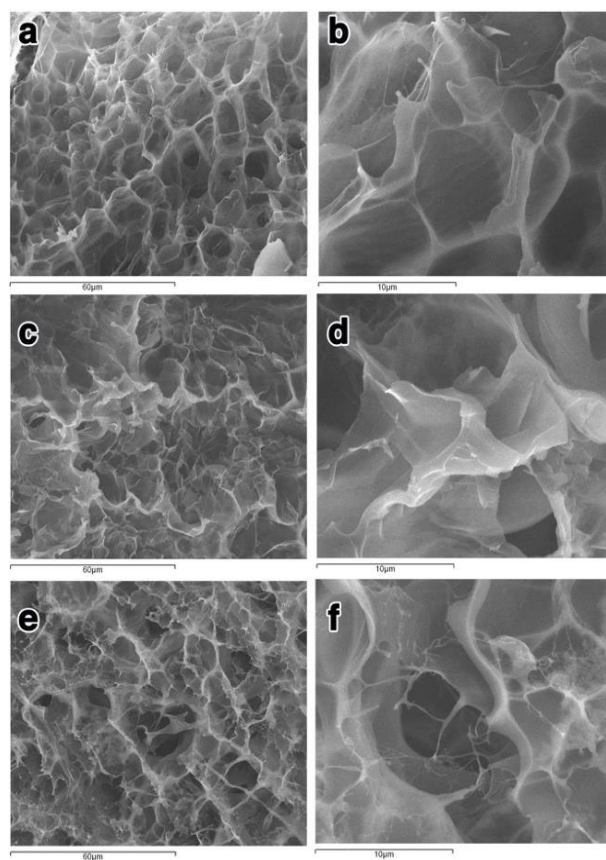


**Fig. 4.** SEM micrographs at different magnifications of GEL (a, b), NP12GEL (c, d) and NP34GEL (e, f).

#### Characterization of hydrogels:

The morphology of the hydrogels was investigated by means of Scanning Electron Microscopy on metal-coated freeze-dried xerogels. The results are shown in **Fig. 4**, where the three different samples can be directly compared at the same magnification along the same column. Micrographs at lower magnification (left column, a, c and e) demonstrate that the typical

porosities present in acrylamide hydrogels (with dimensions ranging between 5 and 10  $\mu\text{m}$ ) are still observed in the hydrogels containing magnetic nanoparticles. Nevertheless, it is clear that the presence of particles takes to a reduced homogeneity and regularity of the porosities. In particular, linear nanostructures are ubiquitously detected in the case of sample NP34GEL, most reasonably because of the tendency of magnetic nanoparticles to self-align to optimize their mutual interaction. Based on these results, we can infer that both NP12 and NP34 can be embedded within acrylamide hydrogels, taking to slightly different morphologies.

The hydrogels were also characterized by means of DSC to investigate their interaction with water and to assess if the presence of nanoparticles could affect it. In **Fig. 5a** the heating runs in the region around 0  $^{\circ}\text{C}$  are shown. All the three samples display the endothermic peak typical of the fusion of *bulk* water, highlighting that the water sorption ability of acrylamide hydrogels is retained also when magnetic nanoparticles are embedded in the polymeric matrix.

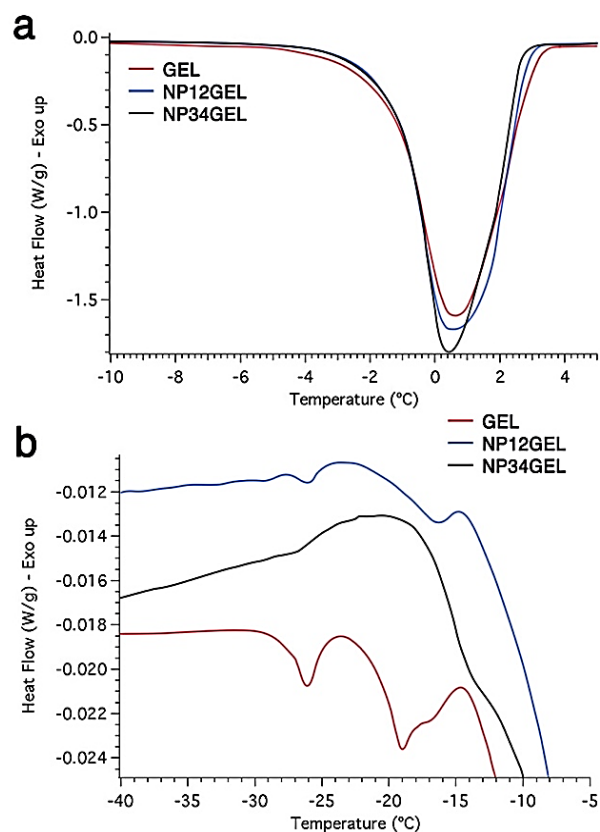


**Fig. 5.** DSC thermograms of hydrogels in the region around 0  $^{\circ}\text{C}$  (a) and in the low temperature region (b).

On the other hand, the thermograms (**Fig. 5b**) significantly differs in the low temperature region (*i.e.*, where the signals related to *confined* water are typically observed). In particular, two peaks are observed at -28  $^{\circ}\text{C}$  and at -20  $^{\circ}\text{C}$  in the sample GEL. To understand the nature of these signals, we compared the hydrogels with their counterparts in terms of composition, but

without sonication during the copolymerization. The SEM micrographs of the reference gel without sonication (see Fig. S7a and S7b) show that the application of ultrasounds takes to an increase of the inhomogeneity in size and shape of the pores. The DSC results of the same sample in the low temperature region (see Fig. S8) show that the reduced homogeneity corresponds to the absence of the peaks observed in the low temperature region for **REFGEL**, clearly suggesting that sonication produces sub-microscopic inhomogeneities where water is confined. These structures are also present in **NP12GEL**, even if to a much smaller extent, while they are not observed in **NP34GEL**, as shown by their DSC thermograms at low temperatures (Fig. 5b). These results suggest that the sonication is much less effective to the hydrogels when magnetic nanostructures are present, as the acoustic waves are most probably absorbed by particle aggregates rather than by the polymeric network. This is consistent with the higher tendency to self-interact by magnetic particles observed by SEM in **NP34GEL**.

## Conclusion

The results reported in this paper demonstrates the viability of a bottom-up synthetic strategy towards the preparation of magnetic nanocomposite materials by sequential reactions with four modular building blocks. In the first step, starting from cobalt ferrite nanoparticles, a divalent molecule was reacted with their surface; in fact, the functionalizing molecule was chosen to possess a carboxylic function and either a terminal alkyne or an azide moiety. The effectiveness of the reaction was studied by means of infrared spectroscopy, showing that an alkaline environment is needed to promote the condensation of the carboxylic group onto the surface of the particle. It is important to highlight that, thanks to the magnetic responsiveness of the particles, the products can be easily recovered simply by magnetic decantation.

In the second step, we took advantage of the introduced alkyne and azide moieties to *click* a second molecule through the Huisgen 1,3-dipolar cycloaddition: in fact, the second molecule is also divalent, as it bears either an azide or a terminal alkyne, respectively, to be exploited in the click chemistry reaction, but also bearing an unsaturated functional group (*i.e.*, a carbon-carbon double bond). The successful preparation of both products was demonstrated by means of infrared spectroscopy and thermogravimetry, taking advantage again of magnetic separation.

In the third step, the functionalized magnetic nanostructures were successfully copolymerized within an acrylamide-based matrix to obtain magnetic hydrogels, whose morphological and water-interaction properties were studied by scanning electron microscopy and differential scanning calorimetry.

The synthetic strategy described in this paper can be used for the inclusion of magnetic nanostructures within

any matrix obtained by radical co-polymerization. Furthermore, it can be easily extended to the design of a large variety of functional composites: in fact, as long as it contains a *clickable* moiety (*i.e.*, a terminal alkyne or an azide group), any molecule could be used during the second step.

## Acknowledgements

This work was supported by CSGI.

## Author's contributions

Conceived the plan: IM, MB, FR, PB; Performed the experiments: IM, MB, FR; Data analysis: IM, MB, FR; Wrote the paper: IM, MB, FR. Authors have no competing financial interests.

## Supporting information

Supporting information are available from VBRI Press.

## References

1. Ridi, F.; Bonini, M.; Baglioni, P., *Adv. Colloid Interface Sci.*, **2014**, *207*, 3.
2. Jeon, I. Y.; Baek, J. B., *Materials*, **2010**, *3*, 3654.
3. Zhu, J.; Wei, S.; Chen, M.; Gu, H.; Rapole, S.B.; Pallavkar, S.; Ho, T.C.; Hopper, J.; Guo Z., *Adv. Powder Technol.*, **2013**, *24*, 459.
4. Tempesti, P.; Bonini, M.; Ridi, F.; Baglioni, P., *J. Mater. Chem. A*, **2014**, *2*, 1980.
5. Arruebo, M.; Fernández-Pacheco, R.; Ibarra, MR.; Santamaría, J., *Nano Today*, **2007**, *2*, 22.
6. Banchelli, M.; Nappini, S.; Montis, C.; Bonini, M.; Canton, P.; Berti, D.; Baglioni, P., *Phys Chem Chem Phys*, **2014**, *16*, 10023.
7. Bonini, M.; Berti, D.; Baglioni, P., *Curr Opin Colloid Interface Sci.*, **2013**, *18*, 459.
8. Brazel, C. S., *Pharm Res*, **2009**, *26*, 644.
9. Nappini, S.; Baldelli, Bombelli F.; Bonini, M.; Nordèn, B.; Baglioni, P., *Soft Matter*, **2009**, *6*, 154.
10. Nappini, S.; Bonini, M.; Bombelli, F.B.; Pineider, F.; Sangregorio, C.; Baglioni, P.; Nordèn, B., *Soft Matter*, **2011**, *7*, 1025.
11. Nappini, S.; Bonini, M.; Ridi, F.; Baglioni, P., *Soft Matter*, **2011**, *7*, 4801.
12. Nappini, S.; Fogli, S.; Castroflorio, B.; Bonini, M.; Baldelli Bombelli, F.; Baglioni P., *J. Mater. Chem. B*, **2016**, *4*, 716.
13. Ridi, F.; Meazzini, I.; Castroflorio, B.; Bonini, M.; Berti, D.; Baglioni, P., *Adv. Colloid Interface Sci.*, **2017**, *244*, 281.
14. Bonini, M.; Lenz, S.; Giorgi, R.; Baglioni, P., *Langmuir*, **2007**, *23*, 8681.
15. Carretti, E.; Bonini, M.; Dei, L.; Berrie, B.H.; Angelova, L.V.; Baglioni, P.; Weiss, R. G., *Acc. Chem Res.*, **2010**, *43*, 751.
16. Kumar, CSSR; Mohammad, F., *Adv. Drug Deliv. Rev.*, **2011**, *63*, 789.
17. Kolb, H. C.; Finn M. G.; Sharpless K. B., *Angew Chem Int Ed.*, **2001**, *40*, 2004.
18. Kolb, H. C.; Sharpless, K. B., *Drug Discov Today*, **2003**, *8*, 1128.
19. Bonini, M.; Wiedenmann, A.; Baglioni, P., *J. Appl Crystallogr*, **2007**, *40*, 254.
20. Rostovtsev, V. V.; Green, L. G.; Fokin, V. V.; Sharpless, K. B., *Angew Chem Int Ed.*, **2002**, *114*, 2708.
21. Bonini, M.; Wiedenmann, A.; Baglioni, P., *J. Phys. Chem. B*, **2004**, *108*, 14901.